

Full Paper

Ag/Pt Core-Shell Nanoparticles on Graphene Nanocomposite for Effective Anodic Fuels Electro-oxidation

Laleh Hosseinzadeh,^{1,*} and Mohammad Mazloum-Ardakani²

¹*Department of Chemistry, Dehloran Branch, Islamic Azad University, Dehloran, Iran*

²*Department of Chemistry, Faculty of Science, Yazd University, Yazd, 89195-741, Iran*

*Corresponding Author,

E-Mail: l.hosseinzadeh2011@gmail.com

Received: 16 December 2019 / Received in revised form: 5 June 2020 /

Accepted: 5 June 2020 / Published online: 30 June 2020

Abstract- The nanocomposite consists of the Ag as a core and Pt as shell on the surface of graphene nanosheets (Ag/Pt-G) was synthesized with a simple method and used as a novel electrochemical platform for an efficient catalyst for oxidation of the ethanol, methanol and formic acid. The morphology and electrochemical properties of Ag/Pt-G nanocomposite were investigated by TEM, X-ray diffraction, and voltammetric methods. Based on experimental results, Ag/Pt-G nanocomposite shows high performance toward oxidation of formic acid, ethanol, and methanol, due to the synergistic effect of Pt, Ag, and graphene nanosheets. The presence of Ag in the structure of nanocomposite leads to enhancing the usage of Pt in the core-shell structure. The proposed nanocomposite with good stability and high catalytic activity can be applied as an effective catalyst.

Keywords- Bimetallic core-shell nanoparticles; Graphene nanosheets; Fuel cell; Formic acid; Methanol; Ethanol

1. INTRODUCTION

Fuel cells as the effective energy sources for transportation have received significant attention [1–3]. Among of various fuel cells, the fuel cells based on the methanol, ethanol and formic acid have attracted great attention due to distinctive properties such as low operating temperature, environmental compatibility, fast recharging, and relatively simple instruments

[4–6]. Recently, the nanomaterials in various field such as catalyst, photo-catalyst, and antibacterial agents have created significant changes [7–11]. Platinum and its alloy nanoparticles have electrocatalyst activity for ethanol, methanol, and formic acid oxidation. Since platinum is expensive and scarce, scientists have made numerous efforts to reduce the Pt amount with enhancing the catalytic efficiency in catalysts based on Pt [12,13]. In general, alkaline media as compared with acidic media presents some advantages for the oxidation of ethanol and methanol. The alkaline media shows higher electrocatalytic activity for oxidation of alcohols and higher current density was obtained. On the other hand, the nanocomposite based on Pt compound has greater reaction kinetics in alkaline media [14,15].

Nowadays, the various nanomaterials were used for enhancement of the sensitivity of sensors, because of their unique advantages and possibilities of a combination of these advantages by the fabrication of nanocomposites. Reduced graphene oxide (RG) has been extensively used for the construction of catalyst. The catalysts based on RG were widely used due to the large surface for supporting various nanoparticles. Therefore, several nanostructure materials such as metal nanoparticles, bimetals, and nanosheets have been used to develop new nanocomposites based on RG [16–20]. Among this nanocomposite, bimetallic core-shell nanoparticles have attracted attention due to the excellent electrocatalytic properties [21,22]. For example, core-shell structure based on the ruthenium and platinum has been applied for the electro-oxidation of methanol [23]. The composite material consists of platinum on aluminum hydroxide oxide and SiO₂ has been applied as an effective catalyst for methanol oxidation [24]. The catalytic performance of metallic nanoparticles is hardly dependent on the size and shape of nanoparticles. Furthermore, aggregations of these nanoparticles can decrease their electrochemical properties [25–31]. Therefore, appropriate supports such as RG can offer an appropriate surface for the distribution of nanoparticles without any aggregation of them [32,33]. Nanocomposite based on Pt show very interesting catalytic properties. The use of Ag particle in cores which not only increasing the catalytic properties of Pt but also decreases the Pt amount [34,35]. Furthermore, the poisoning of CO-like species at the Pt surface decrease in the presence of Ag in the core-shell structure [4].

These reasons prove that the core-shell nanocomposite consists of the Ag and Pt on the graphene nanosheets (Ag/Pt-G) as an effective catalyst for oxidation of formic acid, methanol, and ethanol. Recently, we have successfully introduced Ag/Pt core-shell-graphene and used for the construction of electrochemical aptasensor for the detection of biomarkers [36]. Herein, the Ag/Pt-G catalyst was successfully synthesized with a simple approach and applied for electrocatalytic oxidation of formic acid, methanol, and ethanol which have a significant attraction in related direct fuel cells.

2. EXPERIMENTAL

2.1. Chemicals

Hexachloroplatinic acid, silver nitrate, hydrazine, ethylene glycol, and sodium borohydride were purchased from Sigma-Aldrich. Hydrogen peroxide, sulfuric acid, hydrochloric acid, sodium hydroxide, phosphoric acid, graphite powder, potassium permanganate, ethanol, sodium citrate, and methanol were obtained from Merck.

2.2. Preparation of nanocomposites

The graphene oxide (GO) was prepared based on a previous report [37]. Based on this method a yellow-brown product was obtained. For the synthesis of Ag/Pt-G, 16 mg of graphene oxide in 15 mL water was sonicated for 1 h. Then, 2.5 mg AgNO₃ was added to the obtained GO suspense. Subsequently, 70 µL of sodium citrate (40 mM) was added. Then, 2 mL of a sodium borohydride solution (2 mM) was added. Next, the product was collected by centrifugation. The powder was dispersed in a mixture of 5 mL ethylene glycol and 5 mL H₂O. After that, 0.1 mL of hexachloroplatinic acid (8 % in H₂O) was added to the obtained suspension. Then, the NaOH solution was added until pH reaches 8. The obtained suspension was stirred at 95°C (240 min). Finally, the product was collected, washed, and dried overnight at 170°C in a vacuum oven.

2.3. Electrochemical measurement

The electrochemical investigation of the synthesized nanocomposite was accomplished with a PGSTAT-302N (Metrohm Autolab, Netherlands). A three-electrode system was used, where a glassy carbon electrode (GC) served as the working electrode, a platinum wire as the counter electrode and an Ag/AgCl/KCl (3.0 M) electrode as the reference electrode. For the modification of electrode, 1 mg of nanocomposite was dispersed in 0.5 mL ethanol. Then, 5.0 µL of suspension was cast onto the GC and dried.

3. RESULTS AND DISCUSSION

3.1. Characterization of nanocomposite

The Ag/Pt-G nanocomposite was investigated with TEM, SEM, and XRD. As can be seen in Fig. 1, the Ag/Pt nanoparticles are decorated on the surface of the graphene nanosheets with nearly uniform size. In these structures, graphene can avoid aggregation of Ag/Pt nanoparticles, and uniform distribution of Ag/Pt on the graphene was obtained. In the obtained Ag/Pt nanoparticle structure, the core (Pt NPs) is darker than shell (Ag NPs). In Fig. 1C, graphene nanosheets exhibited a morphology consisting of a thin wrinkling paper-like structure.

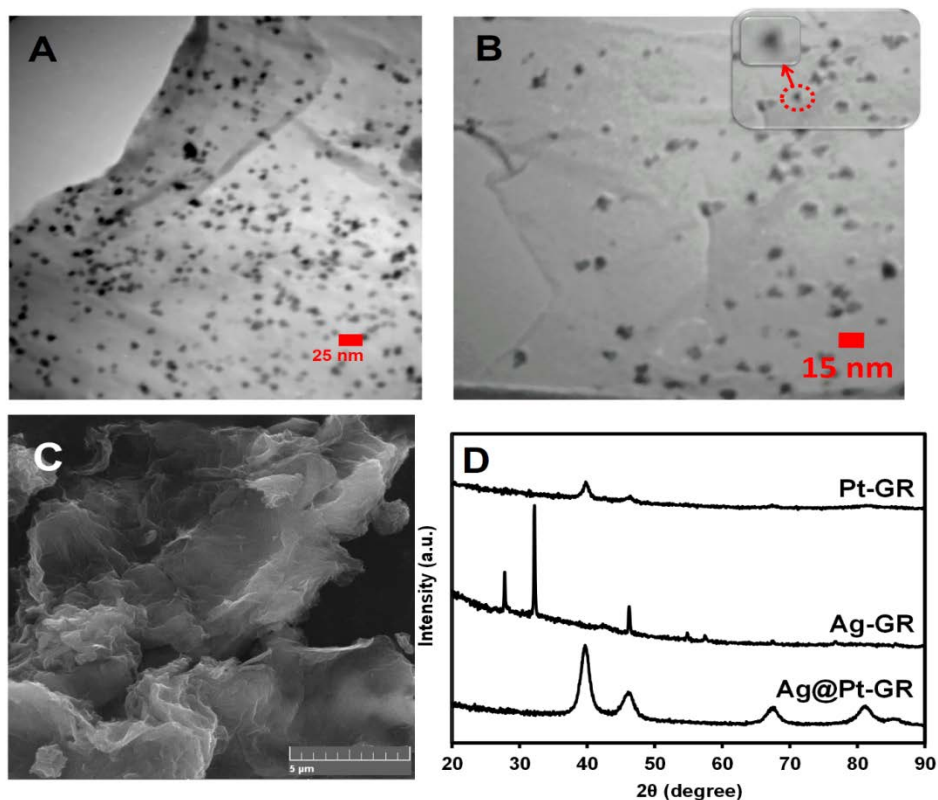


Fig. 1. (A, B) TEM image of Ag/Pt-G nanocomposite, (C) SEM image of G, (D) XRD patterns of Pt-G, Ag-G and Ag/Pt-G

Fig. 1D shows the typical XRD patterns of Pt-G, Ag-G and Ag/Pt-G nanocomposite (Fig 1D). In Pt-G pattern, the peaks at 2θ values of 39.8° , 46.3° , 67.4° and 81.4° assigns to the planes (111), (200), (220), and (311), respectively, indicates that Pt is successfully loaded on the graphene nanosheets. In Ag-G pattern, the peaks at 32.2° , 46.2° , 67.4° and 76.7° assigns to the planes (111), (200), (220), and (311), respectively [38]. The peaks of the Ag/Pt-G nanocomposite were located between the peaks of Pt and Ag, suggesting that Ag/Pt nanoparticles were obtained. No diffraction peaks assign to the Ag are observed in Ag/Pt-G diagram. These results indicate that the surface of the core in core-shell structure covered by Pt.

The oxygen-containing groups of the graphene oxide could adsorb silver ions by electrostatic interaction and the next silver ions were reduced with the reducing agents. The graphene oxide provides a large surface for Ag nanoparticles. The Ag nanoparticles were covered with Pt shell due to the strong interaction between the Pt and Ag than that between the Pt and graphite. Furthermore, these metals have an fcc structure, therefore, Pt prefers the covers of Ag in the Ag/Pt structure [39,40].

3.2. Electrochemical measurement

For the investigation of electrochemical properties of Ag/Pt-G toward ethanol, CVs

technique was performed from -800 mV to 200 mV (Fig. 2). For the comparison, the background CVs of GC and Ag/Pt-G in 1.0 M sodium hydroxide was reported. Then, ethanol oxidation was also investigated at the various modified electrode. Based on the presented voltammograms, the electrocatalytic oxidation currents were observed only at Pt-G and Ag/Pt-G, while the current density of in the presence of Ag is higher than Pt-G. This could be attributed to the nanocomposite structure. The use of Ag nanoparticle in cores was enhancing the Pt catalytic properties for ethanol oxidation, due to the compact and pinhole-free Pt layer. The anodic peak is observed in the reverse scan, which was related to the separation of the incompletely oxidized carbonaceous intermediates [41].

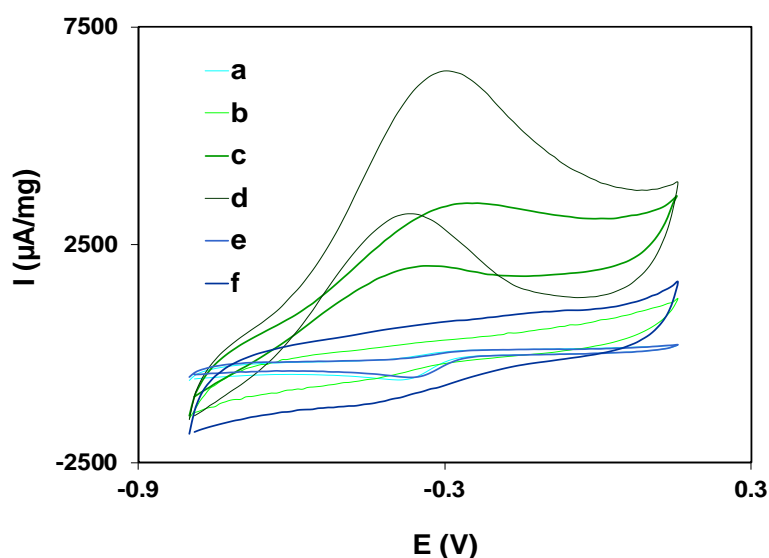


Fig. 2. CVs of (a) GC, (b) G/GC, (c) Pt-G/GC and (d) Ag/Pt-G/GC 1 M ethanol & 1 M NaOH solution. (e) GC and (d) Ag/Pt-G/GC in 1 M NaOH solution. Scan rate is 100 mV/s

The I_f/I_b ratio (forward oxidation current / reverse anodic current) was calculated to be 2.1 and 1.7 for Pt-G and Ag/Pt-G, respectively. The better tolerance to the poisoning species during the ethanol oxidation occurs in the higher I_f/I_b ratio. These results indicate that, in the forward scan, a higher amount of carbonaceous intermediates was oxidized for Ag/Pt-G compared to Pt-G. Therefore, Ag/Pt-G exhibits more significant catalytic activity toward ethanol electro-oxidation.

Fig. 3A displays the CVs of the Ag/Pt-G in 1 M ethanol in various scan rates. The inset of Fig. 3A shows that the I_p increases linearly dependent on the scan rate ($v^{1/2}$) [42]. Therefore, the electro-oxidation of ethanol on Ag/Pt-G could be a diffusion-controlled process.

Fig. 3B shows performing successive CVs of Ag/Pt-G in 1 M ethanol. After 60 cycles, the peaks currents of Ag/Pt-G for ethanol increase clearly by the increase of the cycle numbers. After reaching to highest peak current in 60th cycles, the peak current starts to

decrease slowly. The increasing forward peak currents are due to the activation of Ag/Pt-G with cycling.

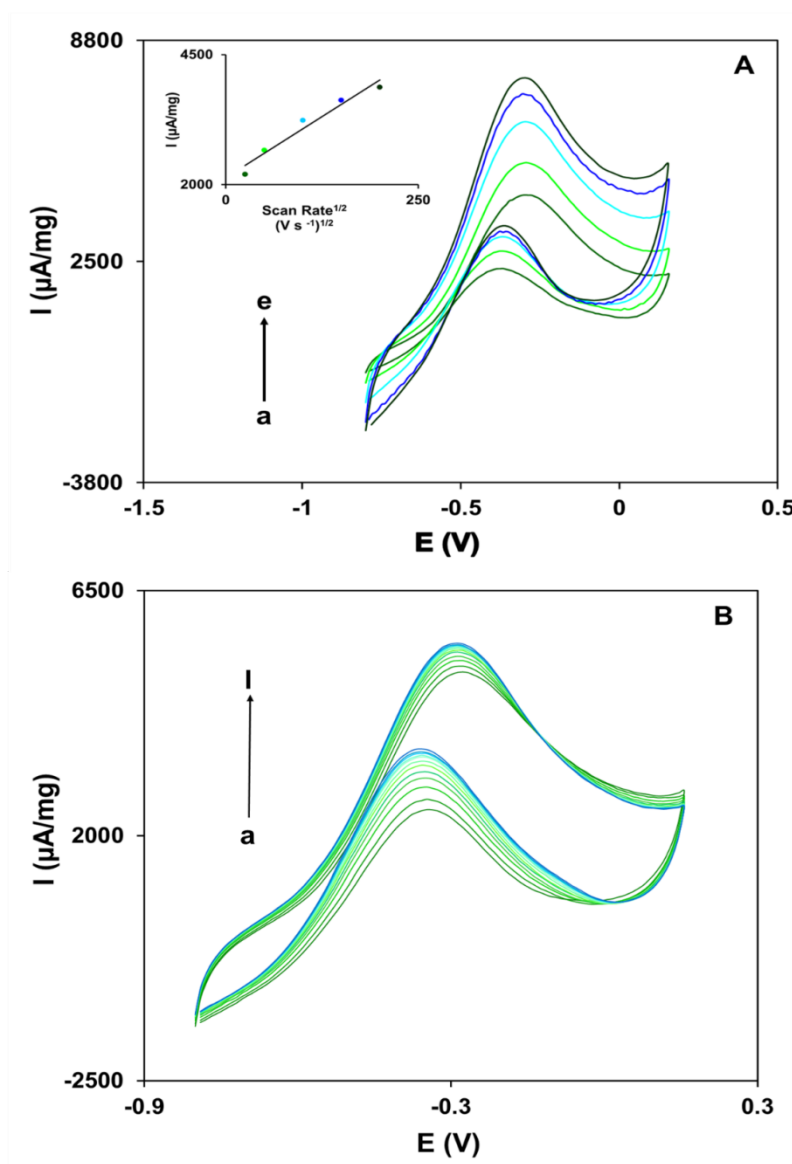


Fig. 3. (A) CVs of the Ag/Pt-G in 1 M ethanol & 1 M NaOH solution at different scan rates, from a to e: 25, 50, 100, 150, 200 and 300 mV s^{-1} , respectively. Inset: plot of the variation of I_p vs. $v^{1/2}$. (B) The CVs as a function of scan cycles, from a to l: 1, 5, 10, 15, 20, 25, 30, 35, 40, 45, 50 and 60th cycles

Furthermore, the collection of carbonaceous species leads to increases in the peak current on the reverse scan [43]. The decreasing of ethanol oxidation current can be due to the decomposition of ethanol during the longtime scans and the poisoning of the Ag/Pt surface.

The repeatability of the nanocomposite was estimated with CVs in 1 M ethanol. The Ag/Pt-G showed repeatability with an RSD of 2.7% for 10 successive assays. The Ag/Pt-G

composite keeps more than 97.8% of its starting current to the electro-oxidation of ethanol after 20-day storage.

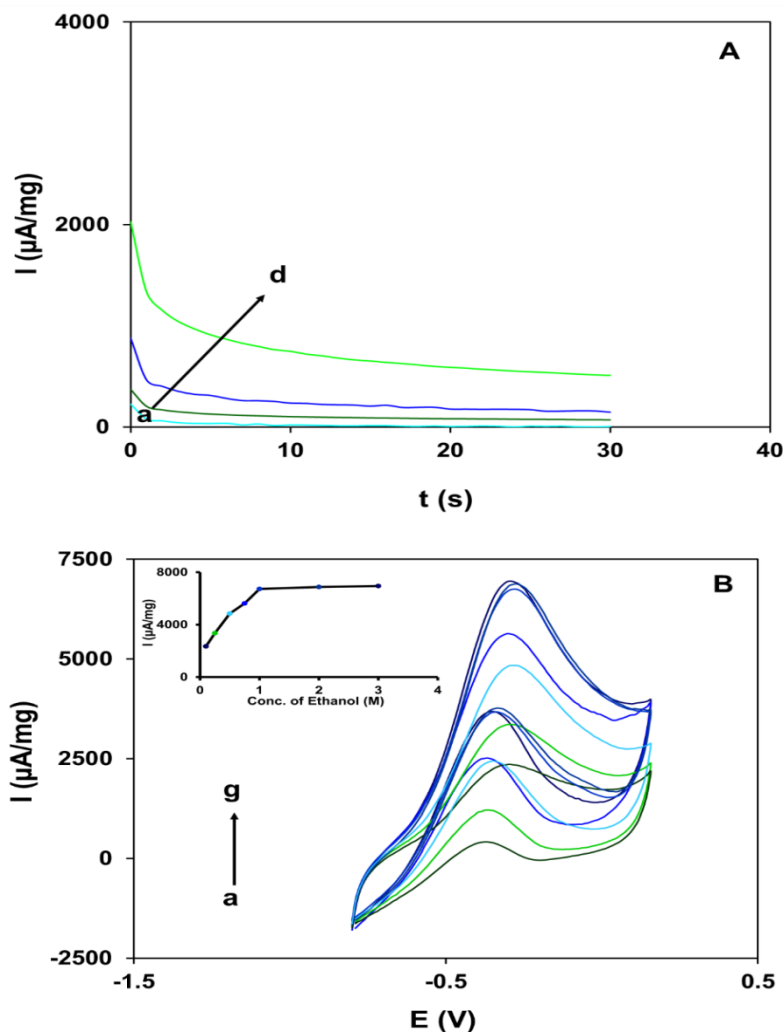


Fig. 4. (A) Chronoamperograms of ethanol oxidation on (a) GC, (b) G/GC, (c) Pt-G/GC and (d) Ag/Pt-G/GC in 1 M ethanol & 1 M NaOH solution. (B) CVs of Ag/Pt-G/GC in 1 M NaOH solution with different concentrations of methanol, from a to g: 0.1, 0.25, 0.5, 0.75, 1, 2 and 3 M, respectively. Scan rate is 100 mV/s. Inset: plot of the dependence of ethanol oxidation peak current vs. the ethanol concentration

Fig. 4A shows the results of chronoamperometry curves of the 1 M ethanol at GC electrode, G/GC, Pt-G/GC, and Ag/Pt-G/GC electrodes. Based on the obtained curves shown in Fig. 4A, the current decreased rapidly which can be due to the carbonaceous intermediates accumulated on the surface. All modified electrode (Fig. 4A) shows a stable current response within ~30 s. It can be seen that the Ag/Pt-G composite shows a higher catalytic current, which is also in agreement with the CV investigation.

Fig. 4B shows the CVs of Ag/Pt-G composite at various concentrations of ethanol were obtained in the potential range of -0.8 V to 0.15 V. As shown in Fig. 4B, the I_{pf} increased

with the increment of ethanol concentration until 1.0 M. There is no change in I_{pt} for a concentration of ethanol above 1.0 M, which is due to the impregnation of the surface at the composite.

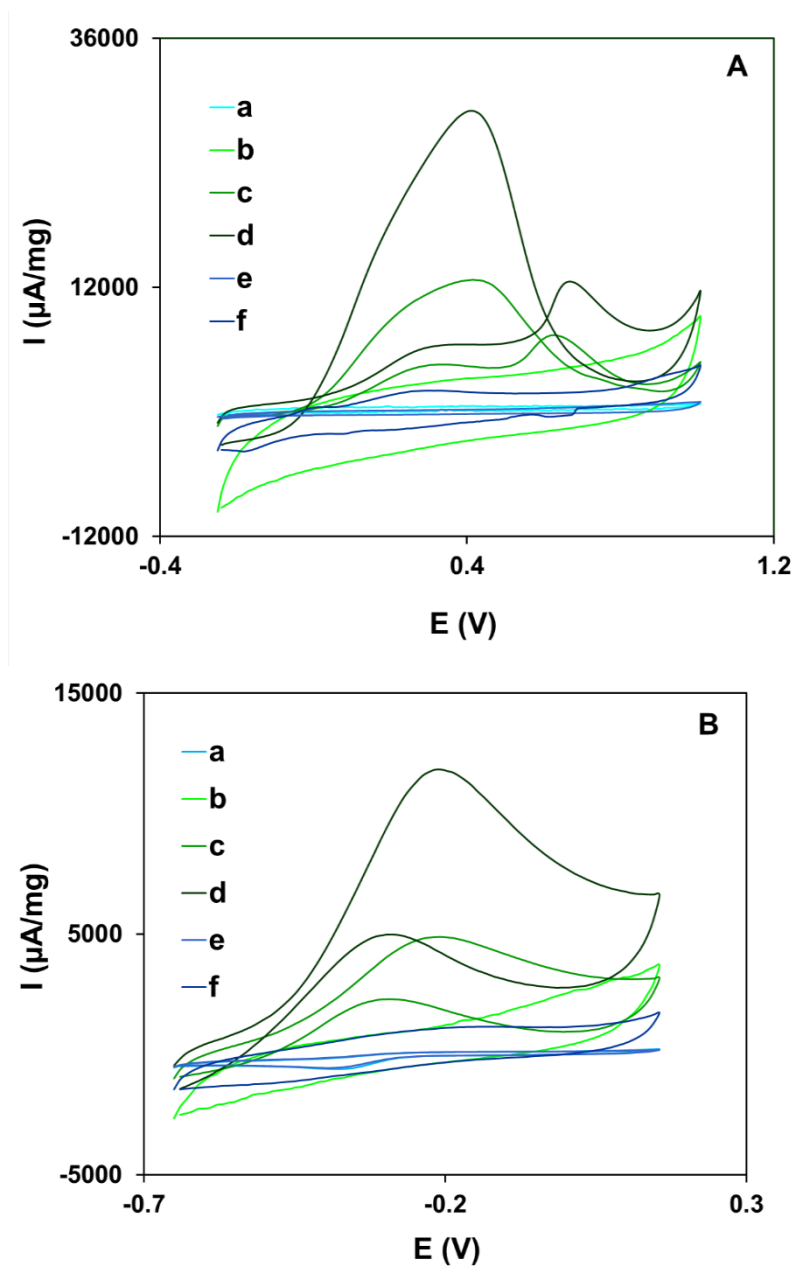


Fig. 5. CVs of (a) GC, (b) G/GC, (c) Pt-G/GC and (d) Ag/Pt-G/GC 1 M ethanol & 1 M NaOH solution. (e) GC and (d) Ag/Pt-G/GC in: **(A)** 0.5 M formic acid & 0.5 M H_2SO_4 solution **(B)** in methanol & 1 M NaOH solution. Scan rate is 100 mV/s

To explore the more desirable electrocatalytic activities of Ag/Pt-G/GC electrode, electrocatalytic oxidation of methanol and formic acid was also investigated by CV. Fig. 5A display CVs of various modified GC electrode in 0.5 M formic acid and 0.5 M H_2SO_4 . The forward peak currents show the catalytic effect of the proposed composite. The results

shown, the electrocatalytic effect in the presence of Ag shell (Ag/Pt-G) is better than Pt-G composite. The forward oxidation peaks in 0.31 and 0.67 V are related to the electro-oxidation of formic acid via the dehydrogenation formic acid and oxidation of CO_{ad} intermediate formed via dehydration formic acid, respectively. The peak in 0.41 V is related to the oxidation of intermediates created in the electro-oxidation of formic acid [2,44].

For methanol electro-oxidation, 1.0 M sodium hydroxide solutions were used as supporting electrolyte and cyclic voltammograms of the various modified electrode by proposed composite in were reported. The forward oxidation peak is due to the electro-oxidation of chemisorbed methanol and the reverse anodic peak is due to the re-oxidation of carbonaceous materials that are incompletely oxidized on the forward scan [4]. In Fig.5B, the highest intensity of the forward oxidation peak current compared with other modified electrodes indicated the performance of Ag/Pt-G composite for methanol electro-oxidation. The above results proposed that the as-synthesized Ag/Pt-G composite is applicable electro-catalysts in a fuel cell for effective electro-oxidation.

4. CONCLUSION

The Ag/Pt-G nanocomposite was synthesized using a simple stepwise procedure. The Ag/Pt-G composite is able to take the excellent catalytic property of each component and was investigated by TEM, X-ray diffraction, and voltammetry techniques. Electrochemical investigations show the high electrocatalytic activities for oxidation of ethanol, methanol in alkaline media and formic acid in acidic media. After adding Ag to Pt-G composite, the I_f/I_b ratio was increased from 1.7 to 2.1, which indicate that, in the forward scan, a higher amount of carbonaceous intermediates was oxidized for Ag/Pt-G compared to Pt-G. Therefore, Ag/Pt-G exhibits more significant catalytic activity. These nanocomposites show acceptable repeatability with an RSD of 2.7% for 10 successive assays. Furthermore, the Ag/Pt-G composite keeps more than 97.8% of its starting current to the electro-oxidation of ethanol after 20-day storage. These results show the potential of Ag/Pt-G composite as a new catalyst in fuel cells application.

REFERENCES

- [1] L. Tao, S. Dou, Z. Ma, and S. Wang, *Electrochim. Acta* 157 (2015) 46.
- [2] C. Zhai, M. Zhu, D. Bin, F. Ren, C. Wang, P. Yang, and Y. Du, *J. Power Sources* 275 (2015) 483.
- [3] L.-L. Wang, J.-L. Wang, Y. Zhang, and R. Feng, *J. Electroanal. Chem.* 759, Part (2015) 174.
- [4] L. Li, M. Chen, G. Huang, N. Yang, L. Zhang, H. Wang, Y. Liu, W. Wang, and J. Gao, *J. Power Sources* 263 (2014) 13.
- [5] M. Mazloum-Ardakani, and A. Khoshroo, *Electrochim. Acta* 103 (2013) 77.

- [6] S. Das, and P.P. Kundu, *RSC Adv.* 5 (2015) 93539.
- [7] M. Rahimi-Nasrabadi, A. Khoshroo, and M. Mazloum-Ardakani, *Sensors Actuators B Chem.* 240 (2017) 125.
- [8] A. Sobhani-Nasab, M. Behpour, M. Rahimi-Nasrabadi, F. Ahmadi, and S. Pourmasoud, *J. Mater. Sci. Mater. Electron.* 30 (2019) 5854.
- [9] S.M. Peymani-Motlagh, A. Sobhani-Nasab, M. Rostami, H. Sobati, M. Eghbali-Arani, M. Fasihi-Ramandi, M.R. Ganjali, and M. Rahimi-Nasrabadi, *J. Mater. Sci. Mater. Electron.* 30 (2019) 6902.
- [10] M. Rahimi-Nasrabadi, F. Ahmadi, and M. Eghbali-Arani, *J. Mater. Sci. Mater. Electron.* 28 (2017) 2415.
- [11] M. Rahimi-Nasrabadi, S.M. Pourmortazavi, M. Aghazadeh, M.R. Ganjali, M.S. Karimi, and P. Novrouzi, *J. Mater. Sci. Mater. Electron.* 28 (2017) 5574.
- [12] A. Khoshroo, L. Hosseinzadeh, A. Sobhani-Nasab, M. Rahimi-Nasrabadi, and H. Ehrlich, *J. Electroanal. Chem.* 823 (2018) 61.
- [13] C. Busó-Rogero, S. Brimaud, J. Solla-Gullon, F.J. Vidal-Iglesias, E. Herrero, R.J. Behm, and J.M. Feliu, *J. Electroanal. Chem.* 763 (2016) 116.
- [14] C. Xu, L. Cheng, P. Shen, and Y. Liu, *Electrochem. Commun.* 9 (2007) 997.
- [15] H. Wang, K. Jiang, Q. Chen, Z. Xie, and W.-B. Cai, *Chem. Commun.* 52 (2016) 374.
- [16] M. Rostami, M. Rahimi-Nasrabadi, M.R. Ganjali, F. Ahmadi, A.F. Shojaei, and M.D. Rafiee, *J. Mater. Sci.* 52 (2017) 7008.
- [17] A. Khoshroo, M. Mazloum-Ardakani, and M. Forat-Yazdi, *Sensors Actuators B Chem.* 255 (2018) 580.
- [18] M.H. Ghanbari, A. Khoshroo, H. Sobati, M.R. Ganjali, M. Rahimi-Nasrabadi, and F. Ahmadi, *Microchem. J.* 147 (2019) 198.
- [19] M.H. Ghanbari, F. Shahdost-Fard, H. Salehzadeh, M.R. Ganjali, M. Iman, M. Rahimi-Nasrabadi, and F. Ahmadi, *Microchim. Acta* 186 (2019) 641.
- [20] E. Sohoul, A.H. Keihan, F. Shahdost-fard, E. Naghian, M.E. Plonska-Brzezinska, M. Rahimi-Nasrabadi, and F. Ahmadi, *Mater. Sci. Eng. C* 110 (2020) 110684.
- [21] F. Ahmadi, T. Mahmoudi-Yamchi, and H. Azizian, *J. Chromatogr. B* 1077 (2018) 52.
- [22] M. Rahimi-Nasrabadi, M.H. Mokarian, M.R. Ganjali, M.A. Kashi, and S.A. Arani, *J. Mater. Sci. Mater. Electron.* 29 (2018) 12126.
- [23] N. Muthuswamy, J.L.G. de la Fuente, D.T. Tran, J. Walmsley, M. Tsytkin, S. Raaen, S. Sunde, M. Rønning, and D. Chen, *Int. J. Hydrogen Energy* 38 (2013) 16631.
- [24] T.H.T. Vu, T.T.T. Tran, H.N.T. Le, L.T. Tran, P.H.T. Nguyen, and N. Essayem, *J. Power Sources* 276 (2015) 340.
- [25] M.A. Marsooli, M. Fasihi-Ramandi, K. Adib, S. Pourmasoud, F. Ahmadi, M.R. Ganjali, A. Sobhani Nasab, M. Rahimi Nasrabadi, and M.E. Plonska-Brzezinska, *Materials (Basel)*. 12 (2019) 3274.

- [26] M. Rahimi-Nasrabadi, S.M. Pourmortazavi, M. Aghazadeh, M.R. Ganjali, M.S. Karimi, and P. Norouzi, *J. Mater. Sci. Mater. Electron.* 28 (2017) 9478.
- [27] M. Rahimi-Nasrabadi, F. Ahmadi, and M. Eghbali-Arani, *J. Mater. Sci. Mater. Electron.* 27 (2016) 13294.
- [28] S.M. Pourmortazavi, M. Rahimi-Nasrabadi, A. Sobhani-Nasab, M.S. Karimi, M.R. Ganjali, and S. Mirsadeghi, *Mater. Res. Express* 6 (2019) 45065.
- [29] S.M. Pourmortazavi, S.S. Hajimirsadeghi, M. Rahimi-Nasrabadi, and M.M. Zahedi, *Mater. Sci. Semicond. Process.* 16 (2013) 131.
- [30] S.M. Pourmortazavi, S.S. Hajimirsadeghi, and M. Rahimi-Nasrabadi, *Mater. Manuf. Process.* 24 (2009) 524.
- [31] M.H. Ghanbari, F. Shahdost-Fard, M. Rostami, A. Khoshroo, A. Sobhani-Nasab, N. Gholipour, H. Salehzadeh, M.R. Ganjali, M. Rahimi-Nasrabadi, and F. Ahmadi, *Microchim. Acta* 186 (2019) 698.
- [32] M. Govindhan, and M. Amiri, A. Chen, *Biosens. Bioelectron.* 66 (2015) 474.
- [33] M. Mazloun-Ardakani, and A. Khoshroo, *Electrochim. Acta* 130 (2014) 634.
- [34] G. Wang, H. Wu, D. Wexler, H. Liu, and O. Savadogo, *J. Alloys Compd.* 503 (2010) L1.
- [35] A. Khoshroo, L. Hosseinzadeh, A. Sobhani-Nasab, M. Rahimi-Nasrabadi, and F. Ahmadi, *Microchem. J.* 145 (2019) 1185.
- [36] M. Mazloun-Ardakani, L. Hosseinzadeh, and Z. Taleat, *Biosens. Bioelectron.* 74 (2015) 30.
- [37] D.C. Marcano, D. V Kosynkin, J.M. Berlin, A. Sinitskii, Z. Sun, A. Slesarev, L.B. Alemany, W. Lu, and J.M. Tour, *ACS Nano* 4 (2010) 4806.
- [38] S. Yu, Q. Lou, K. Han, Z. Wang, and H. Zhu, *Int. J. Hydrogen Energy* 37 (2012) 13365.
- [39] R. Wang, H. Li, H. Feng, H. Wang, and Z. Lei, *J. Power Sources* 195 (2010) 1099.
- [40] M. Rahimi-Nasrabadi, S.M. Pourmortazavi, S.A.S. Shandiz, F. Ahmadi, and H. Batooli, *Nat. Prod. Res.* 28 (2014) 1964.
- [41] R. Mancharan, and J.B. Goodenough, *J. Mater. Chem.* 2 (1992) 875.
- [42] M. Mazloun-Ardakani, L. Hosseinzadeh, A. Khoshroo, H. Naeimi, and M. Moradian, *Electroanalysis* 26 (2014) 275.
- [43] Q. Shi, and S. Mu, *J. Power Sources* 203 (2012) 48.
- [44] C. Venkateswara Rao, C.R. Cabrera, and Y. Ishikawa, *J. Phys. Chem. C* 115 (2011) 21963.